CYTOGENETICS

Molecular cytogenetic characterization of two murine cancer cell lines derived from salivary gland

Ralf Steinacker[1], Thomas Liehr[1], Nadezda Kosyakova[1], Martina Rincic[2], and Shaymaa S. Hussein Azawi[1]

[1]Jena University Hospital, Friedrich Schiller University, Institute of Human Genetics, Am Klinikum 1, D-07747 Jena, Germany
[2]Department for Functional Genomics, Centre for Translational and Clinical Research, University Hospital Centre Zagreb, University of Zagreb School of Medicine, Zagreb, Croatia

Address correspondence and requests for materials to Thomas Liehr, Thomas.Liehr@med.uni-jena.de

Abstract

Here two murine salivary gland cancer (SGC) cell lines WR21 and SCA-9 were studied for the first time in detail by high-resolution molecular cytogenetic approaches. This study revealed that these cell lines are models for human SGCs of initial stage myoepithelioid or mucoepidermoid (WR21) and of advanced stage mucoepidermoid (SCA-9) tumors. Besides, three genes most likely playing a role in SGC development (*FGF10*, *ELAVL1*/*HUR* and *SEL1*) were identified. All of them were involved in translocation events in these in vitro models and thus were most likely activated. Overall, the present study highlights the necessity not only to establish but also to genetically characterize murine tumor cell lines. Without such a characterization they cannot be used in a reasonable way in research.

Keywords: salivary gland cancer (SGC), murine tumor cell lines, WR21, SCA-9, myoepithelioid SGC, mucoepidermoid SGC, *FGF10*, *ELAVL1*/*HUR*, *SEL1*.

Introduction

Salivary gland cancers (SGCs) are a specific and rare subgroup of tumors known from oral and maxillofacial clinical practice. They account for around 3–5 % of all head and neck cancers and for only less than 0.5 % of all cancers (Zboray et al., 2018). Nevertheless, SGCs include more than 35 histological subtypes and are known for their progressive and heterogeneous clinical behavior (El-Naggar et al., 1997; Persson et al., 2009; Cao et al., 2018).

The mentioned subtypes of SGCs exist partially due to the fact that salivary glands consist of three major paired glands (parotid, submandibular and sublingual) and minor glands, located in the mucosa of the palate, lips and respiratory tract (Omitola and Iyogun, 2018; Zboray et al., 2018). Tumors located in the parotid part are only 25 % malignant. However, the incidence of malignancies is much higher in the submandibular part (50 %) and minor salivary glands (60–80 %) (Sood et al., 2016; Solanki, 2011). In general, SGCs are divided in two forms: (i) a simple palpable lump, being well-defined, discrete, and mobile, and (ii) a lump with significant accompanying symptoms like pain, rapid growth, fixity to surrounding structures, nerve involvement and/or neck metastasis (Sood et al., 2016). Current therapeutic options for human SGCs are limited. Depending on their location, some SGCs can be surgically addressed, while others are difficult to remove completely. Radiation therapy is used; still it has turned out to be less effective for clinical treatment. Accordingly, chemotherapy is the only treatment option in metastatic SGCs (Keller et al., 2017; Zboray et al., 2018).

Citation: Steinacker, R., Liehr, T., Kosyakova, N., Rincic, M., and Hussein Azawi, S. S. 2018. Molecular cytogenetic characterization of two murine cancer cell lines derived from salivary gland. Bio. Comm. 63(4): 243–255. https://doi.org/10.21638/spbu03.2018.403

Author's information: Ralf Steinacker; Thomas Liehr, PD, Dr., PhD, Head of Laboratory, orcid.org/0000-0003-1672-3054; Nadezda Kosyakova, MD, PhD, Scientist; Martina Rincic, PhD, Scientist; Shaymaa S. Hussein Azawi, MSc, PhD Student

Manuscript Editor: Alla Krasikova, Saint Petersburg State University, Saint Petersburg, Russia

Received: October 30, 2018;

Revised: November 22, 2018;

Accepted: December 28, 2018;

Funding: This work was supported by Grant No. 2013.032.1 of the Wilhelm Sander-Stiftung.

Competing interests: The authors have declared that no competing interests exist.

The detailed molecular mechanisms controlling tumor progression and metastasis in SGCs and their genetic profiles are still not well understood (Vekony et al., 2009). However, characterization of these underlying mechanisms is essential for understanding and development of more effective methods of diagnosis and treatment against the disease (Murase et al., 2016). Hence, there is a need for better understanding of the genetics and molecular mechanisms of SGC-pathogenesis, to be used in the future toward the development of novel therapeutic approaches (Cao et al., 2018; Murase et al., 2016; Zboray et al., 2018).

One possible approach for studying the biology of SGCs and developing new therapeutic strategies is the use of mouse models (Zboray et al., 2018). Previous research showed that submandibular gland-derived tumor cell lines present characteristics of differentiated epithelial cells and can be used to study proliferation signaling pathways and their regulation (Trzaskawka et al., 2000; Español et al., 2012). Still, surprisingly, murine cell lines used as models for human SGCs have not yet been very well characterized genetically for their tumor-associated alterations.

Fluorescence in situ hybridization (FISH) and microarray-based comparative genomic hybridization (array CGH) were used in this study to determine the genomic aberrations of the two murine SGC cell lines WR21 and SCA-9. WR21 was first described by Young et al. (2006) as being derived from a salivary tumor in a male wap-ras subline 69-2 (C57BL/6, SJL) transgenic mouse; it was already established in 1989. Such tumors are described as extremely aggressive and as expressing high levels of oncogenic ras-protein from the activated human *H-RAS* transgene (Nielsen et al., 1994). SCA-9 was already established in 1980 (Barka, 1980; Barka et al., 2005) and was derived from a carcinogen (7,12-dimethylbenz(a)anthracene) -induced tumor of a male Swiss-Webster mouse submandibular gland. Both cell lines have only been applied in 10 published studies (see Pubmed: https://www.ncbi.nlm.nih.gov/pubmed/?term=wr21 and https://www.ncbi.nlm.nih.gov/pubmed/?term=SCA-9+mouse), which may also be due to the fact that their genetics had not been studied in detail. Here, we analyzed WR21 and SCA-9 cell lines by FISH-banding and aCGH and aligned them with their human SGC subtypes.

Material and Methods

CELL LINES

The cell lines WR21 and SCA-9 were obtained from American Type Culture Collection (ATCC® CRL-2189™, ATCC® CRL-1734™; Middlesex, UK). They are indicated there as 'not further characterized salivary tumor lines' to be grown adherently in DMEM medium containing 10 % fetal calf serum in the presence of antibiotics. For this study, cells were worked up cytogenetically as previously reported (Rhode et al., 2018) and in parallel whole genomic DNA was extracted using the Blood & Cell Culture DNA Midi Kit (Qiagen; Hilden, Germany) according to the manufacturer's instructions and described elsewhere (Kubikova et al., 2017). We conducted molecular cytogenetic analyses on the cell line-derived chromosomes and aCGH analyses on the extracted DNA (see below).

According to the ethical committee (medical faculty) and the Animal Experimentation Commission of the Friedrich Schiller University, there are no ethical agreements necessary for studies involving murine tumor cell lines like WR21 and SCA-9.

MOLECULAR CYTOGENETICS

FISH was performed as previously described (Kubikova et al., 2017). Whole chromosome paints ("SkyPaint™ DNA Kit M-10 for Mouse Chromosomes", Applied Spectral Imaging, Edingen-Neckarhausen, Germany) were used for multicolor-FISH (mFISH), and murine chromosome-specific multicolor banding (mcb) probe mixes for FISH-banding (Liehr et al., 2006). At least 30 metaphases were documented and analyzed for each probe set ((including using SkyPaint™) Zeiss Axioplan microscopy, equipped with ISIS software (MetaSystems, Altlussheim, Germany)). Array-based comparative genomic hybridization (aCGH) was done according to standard procedures by "SurePrint G3 Mouse CGH Microarray, 4×180K" (Agilent Technologies) (Kubikova et al., 2017).

DATA ANALYSIS

The breakpoints and imbalances of WR21 and SCA-9 were determined after analyses of aCGH and mcb data, and aligned to human homologous regions using Ensembl and the UCSC Genome Browser, as previously described (Leibiger et al., 2013). The obtained data were compared to genetic changes known from human SGCs according to Fowler et al. (2006), Rao et al. (2008), Persson et al. (2009), Vekony et al. (2009), Jee et al. (2013) and Matse et al. (2017).

Results

WR21 is mitotically relatively stable, and the near-diploid karyotype has an overall low rate of single cell aberrations; still, it developed two main clones. Clone 1 represents 16.6 % of the cells and has the karyotype 44,XY,+Y,+inv(4)(A1C4),+8,der(9)(A1->E2::E1-qter),der(12)(A1->F2::F1->qter),+19. Clone 2 together with one subclone was found in 83.4 % of the cells. Main-

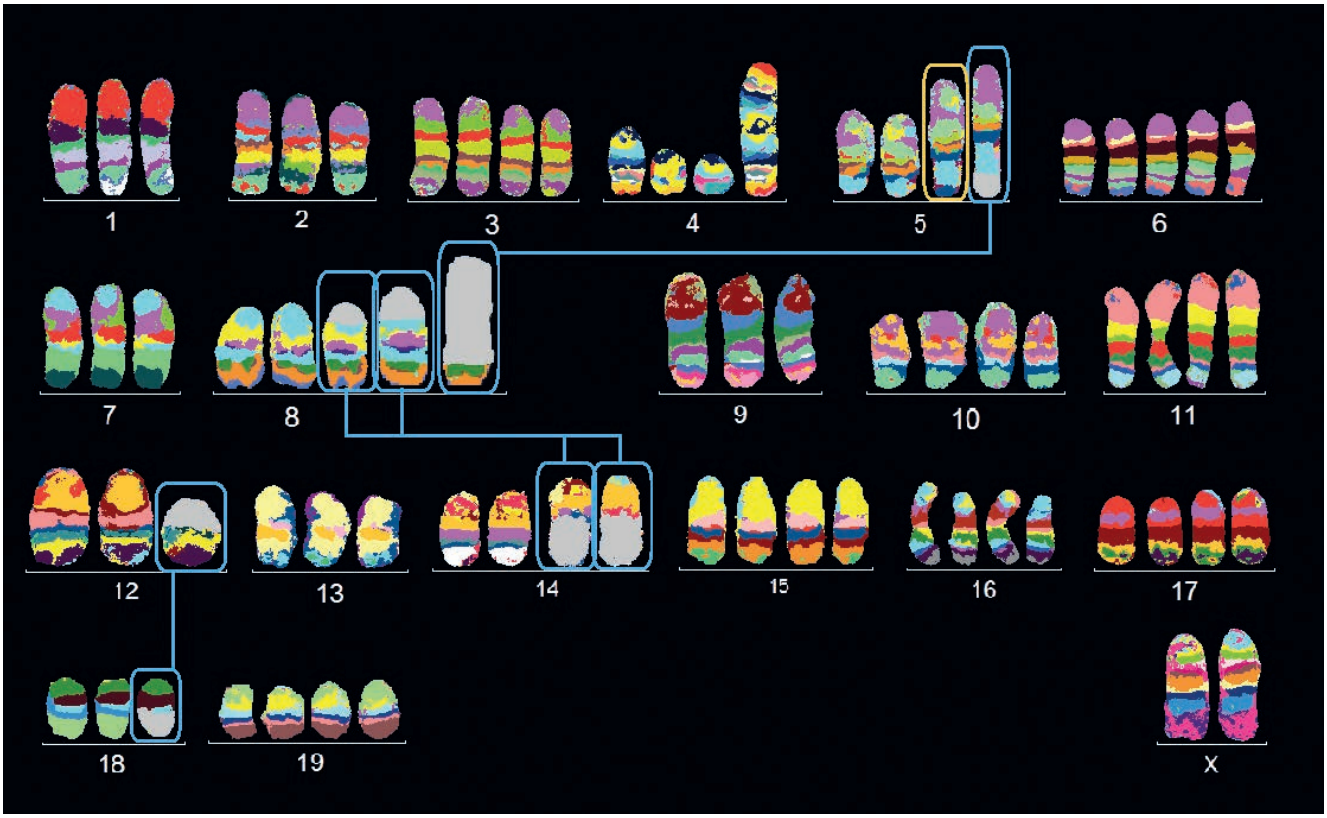

Fig. 1. Murine multicolor banding (mcb) was applied on chromosomes of SGC cell line WR21. Typical pseudocolor banding for all 21 different murine chromosomes is shown for clone 2. This figure depicts the summary of 21 chromosome-specific FISH-experiments. One derivative chromosome consisting of two different chromosomes is highlighted by frames and shown twice in this summarizing karyogram.

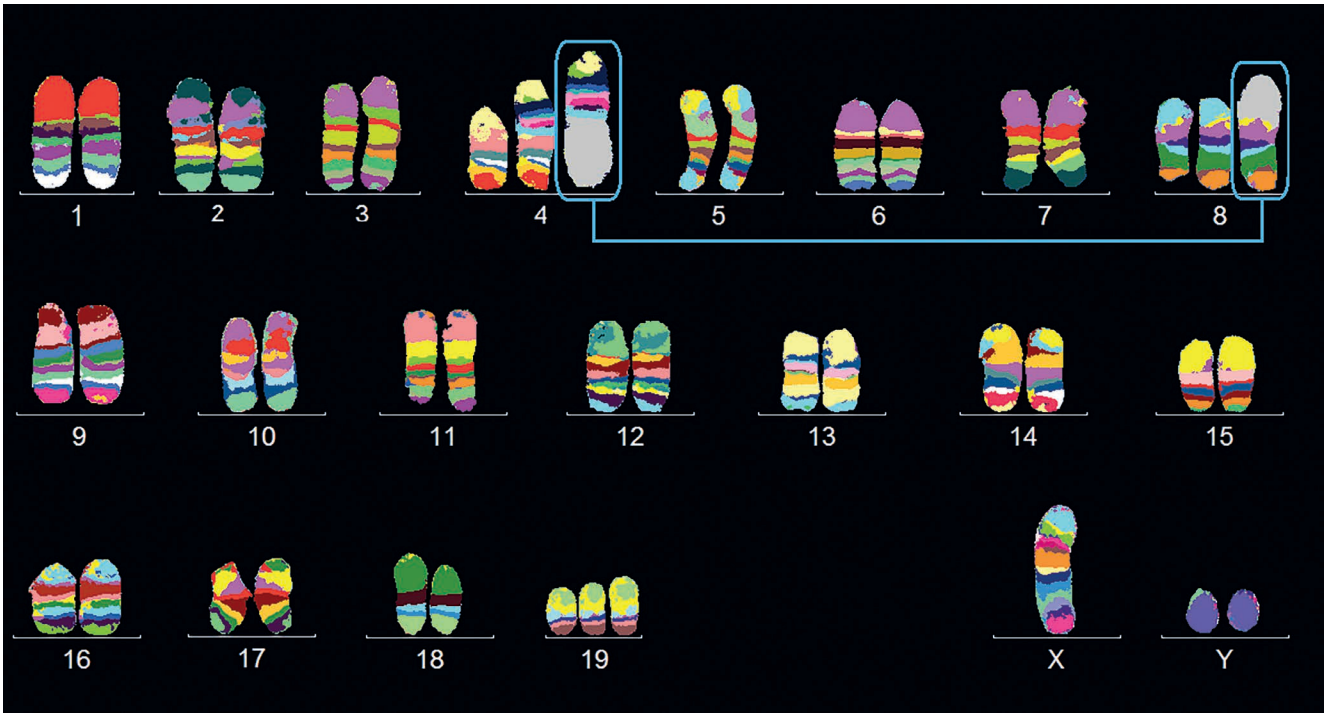

Fig. 2. mcb-results for SGC cell line SCA-9 cell line are shown. Four derivative chromosomes are highlighted by blue frames and shown twice in this summarizing karyogram; the derivative chromosome 5 is highlighted by a yellow frame.

Table 1. Imbalances larger than one cytoband present in WR21 were translated to their corresponding homologous regions in human karyotype (see Suppl. 1) and are listed in the first column. Those are compared to four common types of human SGCs

Chr. region in human	WR21	Adenoid cystic carcinoma	Myoepitheliomas	pleomorphic adenoma	Mucoepidermoid
11q13.3	Gain	Gain			
19p13.2-p13.12	Gain	Gain			
11q12.1-q13.3	Gain	Gain	Gain		Gain
8p23.3-p21.3	Gain		Gain	Loss	Loss
13q33.1-q34	Gain		Gain		Gain
22q12.3	Gain		Gain		
8p12-p11.21	Gain			Gain	
2q22.1-q32.1	Loss			Gain	
19p13.12-p13.11	Gain				Gain
3q25.1-q26.2	Gain				Gain
Overall agreement		**3/10**	**4/10**	**1/10**	**4/10**

Table 2. Imbalances larger than one cytoband present in SCA-9 were translated to their corresponding homologous regions in human karyotype (see Suppl. 2) and are listed in the first column. Those are compared to 4 human SCG-subtypes

Chr. region in human	SCA-9 copy numbers	Adenoid cystic carcinoma	Myoepitheliomas	pleomorphic adenoma	Mucoepidermoid
16p	altered	Gain			Gain
9q33.3-q34.3	altered	Gain			
11q23.3	altered	Gain			
19q13.3-p13.11	altered	Gain			Gain
21q22.3	altered	Gain			
13q21-q22	altered	Loss	Gain		Gain
1p32-p36	altered	Loss			Loss
5q13.2-q15	altered				Loss
3p21.3	altered			Loss	
11pter–p14.3	altered			Loss	
15q25~qter	altered				Gain
6p22~q24	altered				Gain
5pter-p15.31	altered				Gain
9q33.3-q34.3	altered				Gain
18q12.2-qter	altered				Gain
12p13.2	altered				Loss
Overall agreement		**7/16**	**1/16**	**2/16**	**11/16**

clone of clone 2 revealed the karyotype 43,XY,+Y,inv(4)(A1C4),+der(4)t(4;8)(:4C4->4A4::A1-E2),+19 and was present in 77 % of all cells (Fig. 1). In the remaining 6.4 % of the cells, clone 2 further acquired a loss in one of the Y-chromosomes; i.e., there was a del(Y) — this subset was called clone 2a.

In SCA-9 most chromosomes are tetraploid and the cell line is chromosomally instable, as reflected by many single cell aberrations: 62~76,XX,-1,-2,idic(4)(A1;A1),del(4)(C1),del(4)(C1),der(5)(A1->G3::G3->G2:),der(5)t(5;8)(5A1->5G3::5G3->5G2::8B1->8E2),+6,-7,-8,-8,-9,-12,-12,-13,der(14)t(14;8)(C1;A1)x2, der(18)t(18;12)(D;E),-18

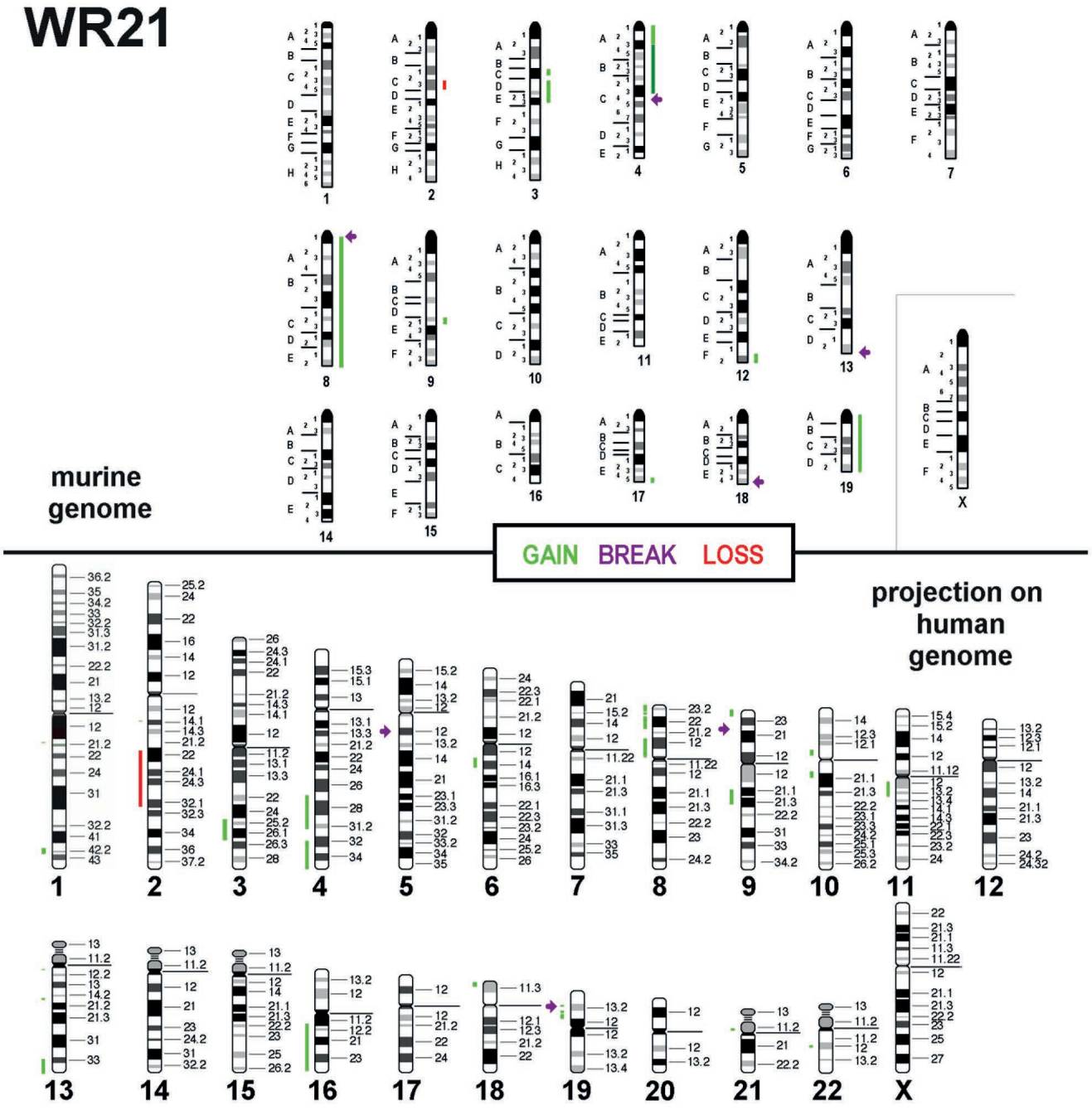

Fig. 3. Imbalances present in WR21 are summarized with respect to a diploid basic karyotype. Gains are depicted as green bars, losses as red bars. In upper part the results are shown for the murine karyotype and in the lower part the translation to human genome. The dark green labeled region of gain at murine chromosome 4 was not detected in aCGH and also not translated to human karyotype.

Most data from the mFISH and mcb for the WR21 and SCA-9 (Table 1) agreed with the aCGH data; the results are shown in Figs. 3 and 4. Some small deletions in murine chromosome 2 and gains in murine chromosomes 3 and 4 (here 4A4 to 4C4, clearly visible mcb) were missed in aCGH. These results were translated to the human genome in the same figures. For this study, imbalances larger than 3.5 megabase pairs were included in the evaluation.

According to the corresponding homologous regions in the human karyotype, we compared the results for both cell lines (Table 1 and 2) with the imbalances for four (adenoid cystic carcinoma, myoepitheliomas, pleomorphic adenoma and mucoepidermoid) of the most common types of SGCs. The highest concordance was found with SGCs of myoepitheliomas and mucoepidermoid for WR21, and of mucoepidermoid for SCA-9.

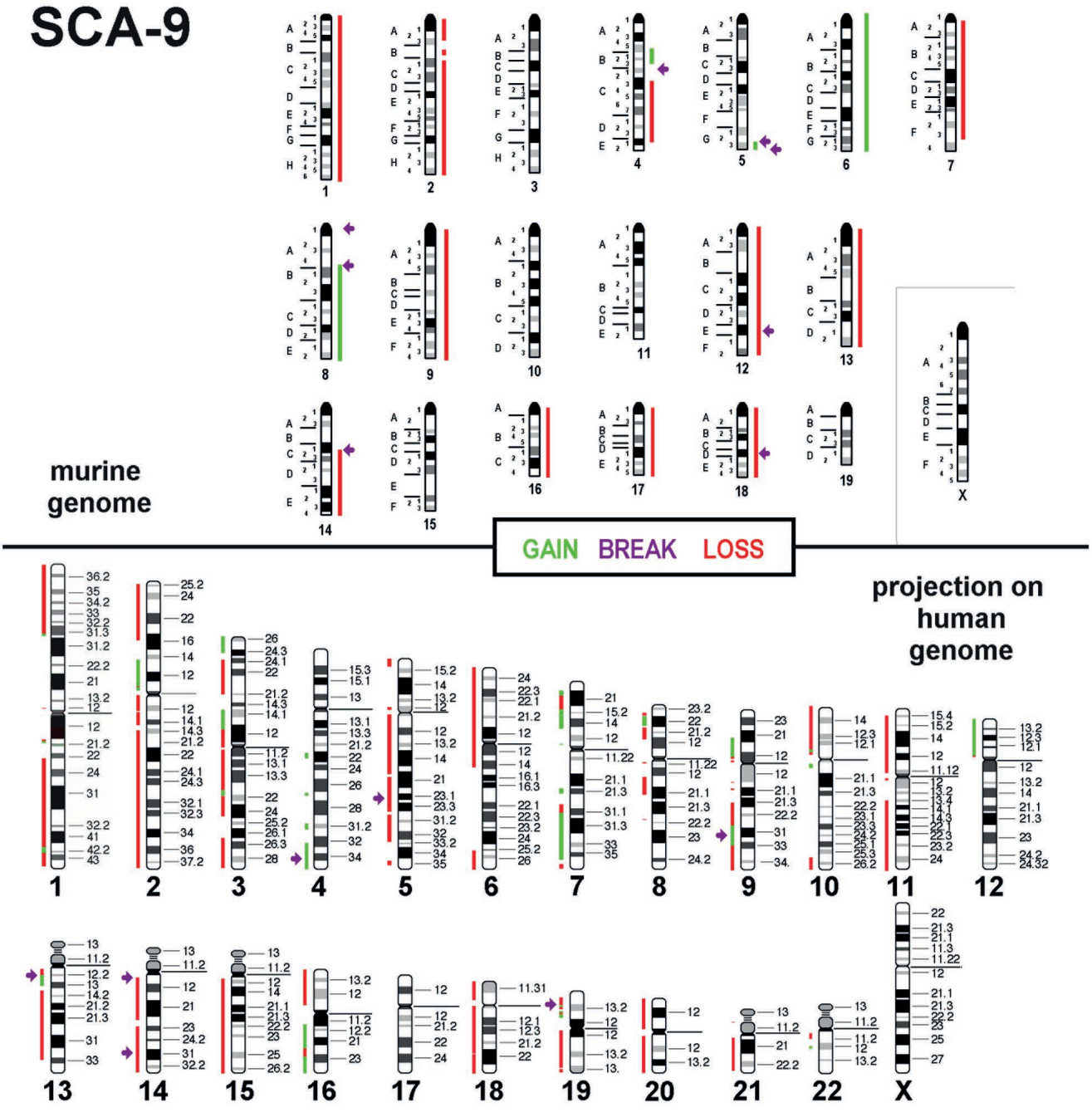

Fig. 4. Imbalances present in SCA 9 are summarized with respect to a tetraploid basic karyotype. Remainder figure as described in legend for Fig. 3.

Discussion

Both the low incidence and heterogeneity of pathology in SGCs explain why this tumor is one of the least studied human cancer types (Seethala, 2017). SGCs present a diverse range of histological and clinical characteristics (Sood et al., 2018). In the literature, there is also significant heterogeneity in the aberrant genetic and molecular pathways described contributing to the development of SGCs (Müller, 2013; Yin and Ha, 2016).

The two murine tumor cell lines which we examined, commercially available as model systems for SGCs, were successfully studied using molecular cytogenetics (mFISH, mcb and aCGH) to provide a comprehensive cytogenetic description regarding ploidy, numerical and structural aberrations and tumor-associated breakpoints, as previously done for other murine tumor cell lines (Leibiger et al., 2013; Kubicova et al., 2017; Guja et al., 2017; Rhode et al., 2018).

In our results, clonal changes with few aberrations from the main clone were observed in both cell lines,

even though two small subclones (denominated as 1 and 2a) were characterizable in WR21 besides one mainline (clone 2). As these cell lines were not karyotyped at the time of establishing, nothing can be stated about karyotypic evolution since then. Considering our own previous studies in other, several decades-old cell lines with known original chromosomal content (Leibiger et al., 2013; Kubicova et al., 2017; Guja et al., 2017; Rhode et al., 2018), all of those were surprisingly stable compared to the original description of the chromosome sets.

Overall, WR21 showed clearly a less aberrant karyotype than SCA-9. Compared to most other solid epithelial tumors, SGCs often were correlated with a normal karyotype or small numbers of chromosomal aberrations (Martins et al., 1995; El Naggar et al., 1997; Hungermann et al., 2002; Vekony et al., 2009), and as expected, salvia carcinomas displayed more chromosomal events than benign tumors from this tissue (Vekony et al., 2009). Thus, WR21 may represent a benign or less advanced cell line than SCA-9. This view is also supported by the fact that polyploidization, i.e. a basic tetraploid karyotype, was observed only in SCA-9, while WR21 was diploid with a gain of only three (derivative) chromosomes. This could be related to telomere-driven tetraploidization in the context of tumor progression (Davoli and de Lange, 2012), but could also be just a cell culture effect (Mastromonaco et al., 2006).

Gains of copy number were observed in both studied cell lines; while gains were more frequent than loss for WR21, the data interpretation used for SCA-9 seems to show a loss rather than a gain of copy numbers. However, this is due to the fact that SCA-9 was interpreted as basically tetraploid — so the high frequency of losses as given in Fig. 4 must consider that this cell line has a massive gain of copy numbers along the entire genome, and the summary in Fig. 4 rather highlights the genomic instability of this cell line.

According to the characterization of WR21 and SCA-9, neither cell line is a model for adenoid cystic carcinomas or pleomorphic adenomas, but most likely for mucoepidermoid SGCs (SCA-9, WR21) and/or myoepitheliomas (WR21 — see Tabs. 1–2).

Interestingly, the breakpoint 13D2 observed in WR21 comprises the gene *FGF10* (see suppl. Tab. 1), which has been associated with salivary gland development (Krejci et al., 2009) and breast cancer (Itoh and Ohta, 2014). Maybe this is a hint that this gene also plays a role in SGCs. For SCA-9 similarly a breakpoint in 8A1 could be associated with the gene *ELAVL1,* also called *HUR,* being described as playing a role in salvia metabolism (Palanisamy et al., 2008) and mucoepidermoid SGC (Cho et al., 2007). The latter confirms that SCA-9 is a model for advanced mucoepidermoid SGC. Another breakpoint (12E) including gene *SEL1* plays a role in the salivary glands of Sjögren's syndrome patients (Barrera et al., 2016).

In conclusion, the present study narrowed down the subtypes of two long established murine cancer cell lines to SGCs of mucoepidermoid (SCA-9, WR21) and/or myoepithelioma (WR21) subtypes and identified three oncogenes potentially playing a role in SGC development. *FGF10*, *ELAVL1*/*HUR* and *SEL1* should be further studied with special attention in SGCs. The chromosomal content of the cells should certainly be controlled before doing extensive further studies, to exclude studying subclones with potentially different and/or advanced karyotypic evolution.

References

Barrera, M. J., Aguilera, S., Castro, I., Cortés, J., Bahamondes, V., Quest, A. F. G., Molina, C., González, S., Hermoso, M., Urzúa, U., Leyton, C. and González, M. J. 2016. Pro-inflammatory cytokines enhance ERAD and ATF6α pathway activity in salivary glands of Sjögren's syndrome patients. *J Autoimmun* 75(1):68–81. https://doi.org/10.1016/j.jaut.2016.07.006

Barka, T. 1980. Biologically active polypeptides in submandibular glands, *J Histochem Cytochem* 28(8):836–859. https://doi.org/10.1177/28.8.7003006

Barka, T., Gresik, E. S. and Miyazaki, Y. 2005. Differentiation of a mouse submandibular gland-derived cell line (SCA) grown on matrigel. *Exp Cell Res* 308(2):394–406. https://doi.org/10.1016/j.yexcr.2005.04.025

Cao, Y., Liu, H., Gao, L., Lu, L., Du, L., Bai, H., Li, J., Said, S., Wang, X., Song, J., Serkova, N., Wei, M., Xiao, J. and Lu, S. 2018. Cooperation between pten and smad4 in murine salivary gland tumor formation and progression. *Neoplasia* 20:764–774. https://doi.org/10.1016/j.neo.2018.05.009

Cho, N. P., Han, H. S., Soh, Y. and Son, H. J. 2007. Overexpression of cyclooxygenase-2 correlates with cytoplasmic HuR expression in salivary mucoepidermoid carcinoma but not in pleomorphic adenoma. *J Oral Pathol Med* 36(5):297–203. https://doi.org/10.1111/j.1600-0714.2007.00526.x

Davoli, T. and de Lange, T. 2012. Telomere-driven tetraploidization occurs in human cells undergoing crisis and promotes transformation of mouse cells. *Cancer Cell* 21(6):765–776. https://doi.org/10.1016/j.ccr.2012.03.044

El-Naggar, A. K., Dinh, M., Tucker, S. L., Gillenwater, A., Luna, M. A. and Batsakis, J. G. 1997. Chromosomal and DNA ploidy characterization of salivary gland neoplasms by combined FISH and flow cytometry. *Hum Pathol* 28(8):881–886. https://doi.org/10.1016/S0046-8177(97)90001-0

Español, A., Dasso, M., Cella, M., Goren, N. and Sales, M. E. 2012. Muscarinic regulation of SCA-9 cell proliferation via nitric oxide synthases, arginases and cyclooxygenases. Role of the nuclear translocation factor-κB. *Eur J Pharmacol* 683(1–3):43–53. https://doi.org/10.1016/j.ejphar.2012.03.013

Fowler, M. H., Fowler, J., Ducatman, B., Barnes, L. and Hunt, J. L. 2006. Malignant mixed tumors of the salivary gland: a study of loss of heterozygosity in tumor suppressor genes. *Mod Pathol* 19(3):350–355. https://doi.org/10.1038/modpathol.3800533

Guja, K., Liehr, T., Rincic, M., Kosyakova, N. and Hussein Azawi, S. S. 2017. Molecular cytogenetic characterization identified the murine B-cell lymphoma cell line A-20 as a model for sporadic Burkitt's lymphoma.

J Histochem Cytochem 65(11):669–677. https://doi.org/10.1369/0022155417731319

Hungermann, D., Roeser, K., Buerger, H., Jakel, T., Loening, T. and Herbst, H. 2002. Relative paucity of gross genetic alterations in myoepitheliomas and myoepithelial carcinomas of salivary glands. *J Pathol* 198(4):487–494. https://doi.org/10.1002/path.1234

Itoh, N. and Ohta, H. 2014. Fgf10: a paracrine-signaling molecule in development, disease, and regenerative medicine. *Curr Mol Med* 14(4):504–509. https://doi.org/10.2174/1566524014666140414204829

Jee, K. J., Persson, M., Heikinheimo, K., Passador-Santos, F., Aro, K., Knuutila, S., Odell, E. W., Mäkitie, A., Sundelin, K., Stenman, G. and Leivo, I. 2013. Genomic profiles and CRTC1–MAML2 fusion distinguish different subtypes of mucoepidermoid carcinoma. *Mod Pathol* 26(2):213–222. https://doi.org/10.1038/modpathol.2012.154

Keller, G., Steinmann, D., Quaas, A., Grünwald, V., Janssen, S. and Hussein, K. 2017. New concepts of personalized therapy in salivary gland carcinomas. *Oral Oncol* 68(1):103–113. https://doi.org/10.1016/j.oraloncology.2017.02.018

Krejci, P., Prochazkova, J., Bryja, V., Kozubik, A. and Wilcox, W. R. 2009. Molecular pathology of the fibroblast growth factor family. *Hum Mutat* 30(9):1245–1255. https://doi.org/10.1002/humu.21067

Kubicova, E., Trifonov, V., Borovecki, F., Liehr, T., Rincic, M., Kosyakova, N. and Hussein, S. S. 2017. First molecular cytogenetic characterization of murine malignant mesothelioma cell line AE17 and in silico translation to the human genome. *Curr Bioinform* 12(1):11–18. https://doi.org/10.2174/1574893611666160606164459

Leibiger, C., Kosyakova, N., Mkrtchyan, H., Glei, M., Trifonov, V. and Liehr, T. 2013. First molecular cytogenetic high resolution characterization of the NIH 3T3 cell line by murine multicolor banding. *J Histochem Cytochem* 61(4):306–312. https://doi.org/10.1369/0022155413476868

Liehr, T., Starke, H., Heller, A., Kosyakova, N., Mrasek, K., Gross, M., Karst, C., Glaser, M., Fickelscher, I., Kuechler, A., Trifonov, V., Romanenko, S. A. and Weise, A. 2006. Multicolor fluorescence in situ hybridization (FISH) applied to FISH-banding. *Cytogenet Genome Res* 114(3–4):240–244. https://doi.org/10.1159/000094207

Mastromonaco, G. F., Perrault, S. D., Betts, D. H. and King, W. A. 2006. Role of chromosome stability and telomere length in the production of viable cell lines for somatic cell nuclear transfer. *BMC Dev Biol* 6(1):41. https://doi.org/10.1186/1471-213X-6-41

Martins, C., Fonseca, I., Felix, A., Roque, L. and Soares, J. 1995. Benign salivary gland tumors: A cytogenetic study of 21 cases. *J Surg Oncol* 60(4):232–237. https://doi.org/10.1002/jso.2930600404

Matse J. H., Veerman E. C. I., Bolscher J. G. M., René Leemans C., Ylstra B. and Bloemena E. 2017. High number of chromosomal copy number aberrations inversely relates to t(11;19)(q21;p13) translocation status in mucoepidermoid carcinoma of the salivary glands. *Oncotarget* 8(41): 69456–69464. https://doi.org/10.18632/oncotarget.17282

Murase, R., Sumida, T., Kawamura, R., Onishi-Ishikawa, A., Hamakawa, H., McAllister, S. D. and Desprez, P. 2016. Suppression of invasion and metastasis in aggressive salivary cancer cells through targeted inhibition of ID1 gene expression. *Cancer Lett* 377(1):11–16. https://doi.org/10.1016/j.canlet.2016.04.021

Müller, S. 2013. An update on salivary gland pathology. *Head Neck Pathol* 7 (Suppl 1):S1–S2. https://doi.org/10.1007/s12105-013-0463-y

Nielsen, L. L., Gurnani, M., Porter, G., Trexler, S., Emerson, D. and Tyler, R. D. 1994. Development of a nude mouse model of ras-mediated neoplasia using WR21 cells from a transgenic mouse salivary tumor. *In Vivo* 8(3):295–302.

Omitola, O. G. and Iyogun, C. A. 2018. Immunohistochemical study of salivary gland tumors in a tertiary institution in South-South Region of Nigeria. *J Oral Maxillofac Pathol* 22(2):163–167. https://doi.org/10.4103/jomfp.JOMFP_108_17

Palanisamy, V., Park, N. J., Wang, J. and Wong, D. T. 2008. AUF1 and HuR proteins stabilize interleukin-8 mRNA in human saliva. *J Dent Res* 87(8):772–776. https://doi.org/10.1177/154405910808700803

Persson, F., Andrén, Y., Winnes, M., Wedell, B., Nordkvist, A., Gudnadottir, G., Dahlenfors, R., Sjögren, H., Mark, J. and Stenman, G. 2009. High-resolution genomic profiling of adenomas and carcinomas of the salivary glands reveals amplification, rearrangement, and fusion of HMGA2. *Genes Chromosomes Cancer* 48(1):69–82. https://doi.org/10.1002/gcc.20619

Rao, P. H., Roberts, D., Zhao, Y., Bell, D., Harris, C. P., Weber, R. S. and El-Naggar, A. K. 2008. Deletion of 1p32-p36 is the most frequent genetic change and poor prognostic marker in adenoid cystic carcinoma of the salivary glands. *Clin Cancer Res* 14(16):5181–5187. https://doi.org/10.1158/1078-0432.CCR-08-0158

Rhode, H., Liehr, T., Kosyakova, N., Rincic, M. and Azawi, S. S. H. 2018. Molecular cytogenetic characterization of two murine colorectal cancer cell lines. *OBM Genetics* 2(3). https://doi.org/10.21926/obm.genet.1803037

Seethala, R. R. 2017. Salivary gland tumors: current concepts and controversies. *Surg Pathol Clin* 10(1):155–176. https://doi.org/10.1016/j.path.2016.11.004

Solanki, G. 2011. Tumors of salivary glands. *IJPR* 1(2):35–38. https://doi.org/10.7439/ijpr.v1i2.355

Sood, S., McGurk, M. and Vaz, F. 2016. Management of salivary gland tumours: United Kingdom national multidisciplinary guidelines. *J Laryngol Otol* 130(S2):S142–S149. https://doi.org/10.1017/S0022215116000566

Trzaskawka, E., Vigo, J., Egea, J.-C., Goldsmith, M.-C., Salmon, J.-M., Deville and De Periere, D. 2000. Cultured tumor cells of murine submandibular gland origin: a model to investigate pHi regulation of salivary cells. *Eur J Oral Sci* 108(1):54–58. https://doi.org/10.1034/j.1600-0722.2000.00670.x

Vekony, H., Röser, K., Löning, T., Ylstra, B., Meijer, G. A., van Wieringen, W. N., van de Wiel, M. A., Carvalho, B., Kok, K., Leemans, S. R., van der Waal, I. and Bloemena, E. 2009. Copy number gain at 8q12.1-q22.1 is associated with a malignant tumor phenotype in salivary gland myoepitheliomas. *Genes Chromosomes Cancer* 48(2):202–212. https://doi.org/10.1002/gcc.20631

Yin, L. X. and Ha, P. K. 2016. Genetic alterations in salivary gland cancers. *Cancer* 122(12):1822–1831. https://doi.org/10.1002/cncr.29890

Young, L. F. and Martin, K. R. 2006. Time-dependent resveratrol-mediated mRNA and protein expression associated with cell cycle in WR-21 cells containing mutated human c-Ha-Ras. *Mol Nutr Food Res* 50(1):70–77. https://doi.org/10.1002/mnfr.200500149

Zboray, K., Mohrherr, J., Stiedl, P., Pranz, K., Wandruszka, L., Grabner, B., Eferl, R., Moriggl, R., Stoiber, D., Sakamoto, K., Wagner, K., Popper, H., Casanova, E. and Moll, H. 2018. AKT3 drives adenoid cystic carcinoma development in salivary glands. *Cancer Med* 7(2):445–453. https://doi.org/10.1002/cam4.1293

Supplement 1. Translation of murine to human data for WR21

region	gain	homologue region in human	
		cytoband	position (GRCh37/hg19)
3D-E3	X1	3q25.1-q26.2	3:149055816-167822106
3C	X1	4q27-q31.1	4:122242382-141190230
8A1–E2	X1	19p13.2 13q33.1-q34 8p23.3-p23.2 8p23.2-p23.1 gap 13q14.3 8p11.23-p11.21 8p11.21 8p12 8p23.1 8p23.1-p22 4q32.2-q35.2 8p22-p21.3 19p13.12-p13.11 22q12.3 4q31.1-q31.23 19p13.2-p13.12 16q11.2-q22.1 16q22.1-q24.3 1q42.13-q42.3 10p11.22-p11.21	19:7112183-8071013 13:103533915-115092930 8:591286-5358752 8:5368147-6693649 13:52435459-53211718 8:36716542-42505949 8:42691750-43058925 8:29190466-36677574 8:8108776-9640417 8:12579073-17958954 4:163504024-190884657 8:18227877-20177976 19:16163040-19774937 22:33658332-35953121 4:141251922-150892329 19:12745060-14683008 16:46693273-69976105 16:70109527-90110030 1:229404294-235324774 10:33112469-35152269
9E1-E2	X1	6q13-q14.3	6:74104388-86360515
12F1-F2	X1	No discerption (Gap)	No discerption (Gap)
19A-D	X1	11q12.1-q13.3 9q21.11-q21.31 2q13 9p24.3-p24.1 10q11.23-q21.1	11:57844834-68709722 9:69086307-82777364 2:114171139-114321953 9:51374-6659223 10:51917603-54540082
17E5	X1	18p11.32	18:861722-2534400
region	**loss**	**homologue region in human**	
		cytoband	**position (GRCh37/hg19)**
2C3	X1	2q22.1-q32.1	2:139292421-187530602
region	breakpoint	homologue region in human	
		cytoband	potential tumor associated genes
4C4	inv.	9p22.3~22.2	*PSIP1*
8A1	t	19p13.2	*ADGRE4P*
13D2	add	5p12	*FGF10*

Supplement 2. Translation of murine to human data for SCA-9

region	gain	homologue region in human	
		cytoband	position (GRCh37/hg19)
4A5-B3	X1	9q22.33-q33.2 9p13.1-p21.2	9:100037894-123488942 9:27325073-38472099
5G2-G3	X2	13q12.13-q13.2 7q21.1-q21.3	13:26784894-34260463 7:97598308-99229367
6A1–qter	x1	7p21.3-p22.1 7q21.2-q21.3 12p11.21 12p11.21 12p11.22-p13.31 12p13.31- p13.33 12p13.31 12p13.33 10q11.21-q11.22 4q27 4q22.1-q22.3 3p25.2-ptr 3p12.3-p14.1 3q21.3 3p25.1-p25.2 3q21.3-q22.1 2p11.2-p13.3 2p11.2 1p31.1 7p14.3-p15.3 7q31.1-q36.1 7q36.1 22q11.11-q11.21	7:7132996-12536829 7:92745197-97502117 12:30985917-31165338 12:31424829-32537434 12:9901365-30943693 12:2903120-7695890 12:8071763-9214464 12:66113-2823666 10:43277986-46218167 4:121018693-122194687 4:89178698-95273100 3:61304-12897767 3:64017713-75322601 3:125725101-129038484 3:12939278-15163105 3:129094932-129632650 2:68715037-87095119 2:88302422-89174373 1:67631910-68317098 7:23254035-33103246 7:112138919-149583263 7:150032467-150558657 22:17565811-18659740
8A4-E2	X1	4q32.2-qtr 4q31.1-q31.23 16q22.1-q24.3 16q11.2-q22.1 1q42.13-q42.3 10q11.21-q11.22 19p13.11-p13.12 19p13.12-p13.2 22q12.3 8p22-23.1	4:163504024-190884657 4:141251922-150892329 16:70109527-90110030 16:46693273-69976105 1:229404294-235324774 10:33112469-35152269 19:16163040-19774937 19:12745060-14683008 22:33658332-35953121 8:12579073-17958954
region	**loss**	**homologue region in human**	
		cytoband	**position (GRCh37/hg19)**
1A2-H6	x1	8q11.21-q12.1 8q13.1-q21.11 6p12.3-p12.2 6q11-q13 6p12.1-p11.2 2q14.3-q21.1 2q11.2-q12.2 13q33.1 2q32.1-q32.2 2q32.2-q37.3 5q21.1 18q21.32-q22.1 2q14.3 2q14.1-q14.3 2q21.2-q22.1 1q32.1-q32.2 1q21.1 1p11.2 1q23.1-q32.1 Yq11.23 1q43-q44 4q26 1q32.2-q42.13	8:50767106-56535248 8:67336477-76107163 6:49796129-52568703 6:61967179-73920868 6:56223874-58686221 2:128848553-131914911 2:97151065-106819719 13:103237605-103533914 2:189007277-190504466 2:190506076-242812118 5:98439740-102728411 18:58351903-65328593 2:122585948-126347698 2:114436107-122578025 2:133138389-138607743 1:206075775-207534964 1:143881371-144095755 1:120754434-120887322 1:158516903-205922697 Y:28358518-28544030 1:240253393-247125743 4:119339188-119512723 1:207575939-227644727

2A1–A3	X1	10q12.1-q15	10:5915452-27157072
2B	X4	2q22.1-q32.1	2:140065297-188395329
2C1-H4	X1	20p13-p11.21 20p13 20q11.21-q13.32 20q13.32-q13.33 15q13.3-q21.2 11q12.1 11q11 11p11.12 11p14.2-p11.2 2q11.1-q11.2 2q13 2p11.2 2q13	20:1736101-25606620 20:102147-1447942 20:29933153-58056214 20:58148222-62907435 15:32906987-51298173 11:56082416-57753858 11:55080583-55323018 11:51377850-51539057 11:26296397-48658712 2:95642277-97040617 2:111483204-112960231 2:87345633-87996071 2:112973390-113650007
4C5-E1	X1	1p32.1-p31.3 1p36.33-p32.2~1	1:59120351-67562260 1:894315-59012766
7A1-F3	X1	19q13.42-q13.43 19q13.43 19q13.31-q13.33 19q12-q13.31 19q12 19q13.33-q13.41 16p13.11 11p15.1-p14.3 15q11.2 15q11.2-q13.1 15q13.1-q13.3 15q26.3 15q26.1-q26.3 15q25.3-q26.1 15q25.1-q25.3 11p11.12 11q13.4-q14.3 10p11.21 11p15.4-p15.1 16p13.11 16p13.11-p12.3 16p12.3-p12.2 16p12.2-p11.2 16p11.2 16p11.2	19:54368915-57485284 19:58523795-59089552 19:45010010-48707700 19:30093064-44860951 19:28589680-30085362 19:48800017-51921957 16:16252815-16388674 11:17403485-25251145 15:22833222-23086601 15:23914751-28586067 15:29107424-32578594 15:99080385-102265870 15:91593058-99078056 15:85829657-91565912 15:80253398-85682414 11:49250334-49827246 11:71627032-89350901 10:37191655-37402201 11:3631069-17360027 16:15260325-15369270 16:16681590-18325190 16:18608156-21351663 16:21572755-28339524 16:28390845-29030948 16:29661006-31520748
9A1-F4		11q14.3-q22.3 19p13.2 7p14.3-p14.2 11q22.3-q25 15q21.2 15q21.2-q25.1 6p12.2-p12.1 6q13-q14.3 15q25.1 3q22.3-q24 3q22.1-q22.3 3p21.31-p21.1 3p24.1-p22.2 3p22.2-p21.31	11:89860533-107436639 19:8919008-11689880 7:33134362-36494039 11:107452617-134843539 15:51349622-51942502 15:51961808-78956872 6:52656530-55784577 6:74104388-86360515 15:79042978-80196839 3:138372654-148087492 3:129931635-138353358 3:46446256-52346387 3:27753690-37261140 3:37269243-46423369
12A1-E	X2	2p25.1-p23.3 2p25.1 2p25.1 2p25.3-p25.1 7q22.3-q31.1 7p21.3-p21.1 7q31.1 14q12-q22.1	2:10303009-26361943 2:9354723-9994801 2:9996101-10284917 2:140908-9278318 7:105210238-107772185 7:12561752-19748810 7:107772206-112136146 14:25157192-52251174
12E–F1	X1	14q23.1-q32.33	14:58666612-106375879
12F1-F2	X2	7q36.3 7p21.1-p15.3	7:157225645-158937901 7:19761201-22528893

13A1-qter	X1	10p15.3-p15.1	10:138698-5865622
		1q42.3-q43	1:235330060-240084659
		7p14.2-p13	7:36524506-43605930
		6p22.3-p22.1	6:20065223-28502803
		6p25.3-p23	6:181261-15099150
		6p23-p22.3	6:15104709-20060798
		9q22.1-q22.32	9:91031851-97067712
		5q35.2-q35.3	5:173750964-177039611
		5q31.1-q31.2	5:134073478-137090938
		9q21.32-q21.33	9:86231955-90340399
		9q22.32-q22.33	9:97320957-99417669
		9p13.1	9:38810965-40707569
		9q12-q13	9:65585614-65901647
		9p11.2	9:43623473-43941731
		8q22.1	8:97247028-97373828
		5p15.33-p15.31	5:191425-7935441
		5q14.3-q15	5:84566270-96144383
		5q13.2-q14.3	5:70265557-84371909
		5q11.1-q13.2	5:49569996-68922426
		1p11.2	1:121149401-121350677
		5p12	5:43446298-46118514
14C1-E5	X2	14q22.1-q23.1	14:52688635-58629894
		14q11.2-q12	14:20211286-24987352
		14q12	14:25040539-25149959
		13q12.12	13:25188452-25511922
		13q12.11	13:20207279-23370461
		13q14.2	13:49821990-50161404
		13q12.13	13:25685086-26668986
		13q12.12	13:23853398-24896355
		13q14.2-q14.3	13:50192169-52356487
		8p23.1	8:9744629-11737304
		8p21.3-p12	8:20206584-29151199
		13q14.11-q14.2	13:41469941-49799059
		13q14.3-q33.1	13:53226033-103089581
16pter-qter	X1	16p13.3-p13.11	16:3283710-15197331
		16p13.11	16:15478874-16187414
		8q11.21	8:48206338-49865275
		12p11.21	12:32634919-33054761
		22q11.21	22:19010381-22338262
		3q27.1-q29	3:182965714-195325931
		3q29	3:195428230-197771581
		3q11.1-q21.2	3:93527487-125343459
		3p12.3-p11.1	3:75865702-90309600
		21q11.2-q22.3	21:15515528-43438088
		21q11.2	21:14535253-14714360
		18p11.21	18:15016525-15155234
		2q21.1	2:132604281-132757591
17A1-E5	X1	6q27	6:167120855-167552070
		6q25.3-q27	6:160103032-166797236
		6q27	6:167859539-170893754
		5q15-q21.1	5:96202316-98405239
		16p13.3	16:222880-3208490
		5q35.1	5:171946752-172722349
		6p21.32-p21.2	6:33359177-39058058
		21q22.3	21:43490502-45122943
		19p13.12	19:15270296-15808207
		19p13.2	19:8366687-8811037
		6p22.1-p21.32	6:29322703-33297218
		6p21.2-p12.3	6:39266498-49681826
		3p25.1-p24.3	3:16307846-20231899
		2q12.2-q12.3	2:107383985-108798215
		19p13.3	19:4229082-6862967
		5q21.1-q22.1	5:102759315-110063021
		18p11.32-p11.22	18:2534401-9972541
		2p23.2-p16.3	2:29033520-51699597
		2p16.3-p16.2	2:51709987-53282184
		18p11.32	18:861722-2534400

18A1–D3	X1	10p11.21 10p12.1-p11.22 10p12.1 10p11.21 18p11.32 18q11.1-q12.3 2q14.3 5q22.1-q22.2 5q31.2-q32 5q22.2-q23.3	10:35284099-35521818 10:28950711-32678701 10:27747786-28722506 10:35676708-37094546 18:112543-599224 18:18528605-41073893 2:127805408-128786667 5:110280120-112296881 5:137225085-147624774 5:112310736-130339352
18D3-qter	X2	5q32-q33.1 18p11.22-p11.21 18q21.31-q21.32 18p11.21 18q12.3-q21.31 18q22.1-q23	5:147647374-150177176 18:10202644-11518916 18:54267924-58201586 18:11649353-13871680 18:41355914-54244819 18:66339761-78010601

region	**breakpoint**	**homologue region in human**	
		cytoband	**potential tumor associated genes**
4C1	del	9q31.3	*AKAP2/ C9orf84*
5G3	dup, inv	7q21.3	*ASNS / BAIAP2L1*
5G2	dup	7q21.3	*ASNS / BAIAP2L1*
8A1	t	19p13.2	*ELAVL1* also called *HUR / FCER2*
8B1	t	4q34.2	*ASB5*
12E	t	14q31.1	*SEL1L / TSHR*
14C1	t	14q22.2	*CGRRF1 / CNIH1 / GCH1 / GMFB*
18D	t	5q23.1	*LOX / FTMT*